Hydrol. Earth Syst. Sci. Discuss., 6, 5631–5664, 2009
www.hydrol-earth-syst-sci-discuss.net/6/5631/2009/

Hydrology and Earth System Sciences Discussions

Papers published in *Hydrology and Earth System Sciences Discussions* are under open-access review for the journal *Hydrology and Earth System Sciences*

A simple two layer model for simulation of adsorbing and nonadsorbing solute transport through field soils

M. S. Akhtar[1], **U. Mohrlok**[2], **and D. Stüben**[3]

[1]PMAS-Arid Agriculture University Rawalpindi, Rawalpindi, Pakistan
[2]Institute for Hydromechanics, University of Karlsruhe, 76131 Karlsruhe, Germany
[3]Institute for Mineralogy and Geochemistry, University of Karlsruhe, 76131 Karlsruhe, Germany

Received: 16 June 2009 – Accepted: 15 July 2009 – Published: 4 September 2009

Correspondence to: M. S. Akhtar (msakhtar@uaar.edu.pk)

Published by Copernicus Publications on behalf of the European Geosciences Union.

Abstract

While rapid movement of solutes through structured soils constitutes the risk of groundwater contamination, simulation of solute transport in field soils is challenging. A modification in an existing preferential flow model was tested using replicated Chloride and Lithium leachings carried out at constant flow rates through four soils differing in grades and type of structure. Flow rates generated by +10 mm, −10 mm, −40 mm, and −100 mm water heads at the surface of 35 cm diameter 50 cm height field columns. Three well-structured silty clay soils under ponding had concurrent breakthrough of Chloride and Lithium within a few cm of drainage, and a delayed and reduced peak concentration of Lithium with decrease in flow rate controlled by the negative heads. Massive sandy loam soil columns had delayed but uniform breakthrough of the solutes over the flow rates. Macropore flow in well-structured silty clay/clay loam soils reduced retardation, R (1.5 to 4.5) and effective porosity, θ_e (0.05 to 0.15), and increased macropore velocity, v_m (20 to 30 cm cm^{-1} drainage) compared to the massive sandy soils. The existing simple preferential flow equation (single layer) fitted the data well only when macropore flow was dominant. The modified preferential flow equations (two layers) fitted equally well both for the adsorbing and nonadsorbing solutes. The later had high goodness of fit for a large number of solute breakthroughs, and gave almost identical retardation coefficient R as that calculated by two-domain CDE. With fewer parameters, the modified preferential flow equation after testing on some rigorous model selection criteria may provide a base for future modeling of chemical transport.

1 Introduction

Rapid movement of solutes to tile-line may transport contaminants to groundwater and, therefore, has been studied extensively. As in field soils, retention of solutes is practically less than the determined values from the batch experiments (Hutchison et al.,

2003; Akhtar et al., 2003b), the arrival time for reactive solutes is the same as that for the nonreactive solutes, e.g. pesticides (Flury et al., 1995; Kung et al., 2000), Phosphorous (Akhtar et al., 2003a), Lithium (Akhtar et al., 2003b), and other cationic and anionic metals (Huber et al., 2004; Akhtar et al., 2009). In this situation, the classical transport models fail to predict arrival time.

Transport parameters are determined using the Convective-Dispersive equation (CDE) which is based on the assumption that solute front moves uniformly (Xue et al., 1997; Mohanty et al., 1998; Elliott et al., 1998; Sarmah et al., 2005). Other models with various degrees of complexity to simulate solute flow in the vadose zone have been tested, e.g. MACRO (Jarvis et al., 1991a,b); USDA's Root Zone Water Quality Model (RZWQM) (Ahuja et al., 2000) and LEACHEM (Hutson and Wagenet, 1995). Conceptually, these models vary mainly in the amount of interaction of solutes with the soil matrix.

As the validity of uniform velocity was questioned (Quisenberry et al., 1994), a two-region mobile-immobile model where total water content is partitioned and a mass transfer function governs the mass exchange between mobile and immobile regions, addressed some of the discrepancies in modelling solute transport in field soils (Jury et al., 1991; van Genuchten, 1991). This approach has been successfully applied in many solute transport studies (Hutchison et al., 2003; McIntosh et al., 1999; Langner et al., 1999; Vervoort et al., 1999; Shaw et al., 2000). However, these models require a large number of parameters. The VS2DT (Lappala et al., 1987), requires a minimum of seven parameters (Zhang et al., 1998) which often lack physical meaning and are difficult to determine independently. Matrix and macropore flows cannot be discriminated easily, thus making hydrological characterization of the two domains uncertain (Castigione et al., 2003). In some cases erroneous parameter estimates have been reported despite high goodness of fit (Akhtar et al., 2003b; Kim et al., 2005).

On the other hand, the preferential flow type equations assume that a surface layer (or a mixing layer) distributes water and solutes into the macropores of the soils' vadose zone (Ritsema and Dekker, 1994; Steenhuis et al., 1994; Jarvis et al., 1991; Ahuja et

al., 2000; Kim et al., 2005). Main differences among various preferential flow models are the assumptions concerning the exchange of solutes with the soil matrix along soil pore wall. The simplest model of Steenhuis et al. (1994) assumes that the flow through the macropores is fast and no interaction takes places with the soil matrix. Other models include some interaction with the matrix (Zhang et al., 1998; Wallach and Steenhuis 1998). Ahuja et al. (2000) assume that some of the solutes end up in dead-end pores. The simple preferential flow model without interaction in the vadose zone has been found fitting only where macropore flow was dominant (Akhtar et al., 2003b). As the model assumes instantaneous mixing, it also failed when mixing and leaching processes occur simultaneously (Mahmood-ul-Hassan et al., 2003).

Following the concept of "mixing" and "transport" layer (Steenhuis et al., 1994), a modified preferential flow type equation was adapted to the experimental conditions where LiCl was applied to intact soil columns at steady state flow conditions. This paper presents fits to the modified preferential flow equation, discusses the variability in the transport parameters, and compares relevant transport parameter with CDE applied with partitioning of water into mobile/immobile regions.

2 Modelling approaches

As several approaches are referred in the literature to describe transport processes in soils with different complexity, this section summarizes the basic principles of the approaches used within this paper.

2.1 Convective Dispersive Equation (CDE)

The CDE model for one-dimensional transport of reactive solutes subject to adsorption in one or two domains has been solved for several boundary conditions given in Parker

and van Genuchten (1984) and other textbooks (Marshall et al., 1996):

$$R\frac{\partial C}{\partial t} = D\frac{\partial^2 C}{\partial x^2} - v\frac{\partial C}{\partial x} \quad (1)$$

where D is the dispersion coefficient [$m^2\,s^{-1}$], $v=q/\theta$ is the mean flow velocity or the transport velocity of a non-adsorbing solute [$m\,s^{-1}$], respectively with the Darcy velocity q [$m\,s^{-1}$] and the volumetric water content θ [$m^3\,m^{-3}$]. The dimensionless retardation factor of the form

$$R = 1 + \frac{\rho K_a}{\theta} \quad (2)$$

(Toride et al., 1999) for adsorbing solute, with a constant adsorption partitioning coefficient K_a [$m^3\,kg^{-1}$] and the bulk density of solid, ρ_b [$kg\,m^{-3}$], scales the solute movement. Thus, the transport velocity is R times lower and arrival time R times longer compared to a non-adsorbed solute.

2.2 Simple preferential flow model

It describes solute transport in natural layered soils by assuming surface soil as a mixing zone and vadose zone as a conveyance zone. The mixing layer is considered as a dynamically behaving reservoir where solute sorption processes and advective transport balance. In the transport layer only a time lag to advective transport occurs. Assuming flow in the mixing zone follows linear reservoir theory, i.e. no interaction with soil matrix in the transport layer (Ritsema and Dekker, 1994) and the applied solute mixes instantaneously, the cumulative loss of solutes, L, [kg] with preferentially moving water through a soil with mixing zone of thickness d [m] is:

$$L = M_0\left[1 - \exp\left(-\frac{Y}{W}\right)\right] \quad (3)$$

(Akhtar et al., 2003b) where M_0 [kg] is the initial mass applied, $W=d\ (\rho_b\ K_a+\theta)$ [m] is the apparent water content; and $Y=qt$ [m] is the cumulative drainage at constant flow rate q since the time t of solute application

2.3 Two layer preferential flow model

Modification in this approach becomes necessary when a solute is injected over a certain time period T_0 [s] into a water flux seeping continuously with a constant specific flow rate q [m s^{-1}], a procedure corresponding to the usual tracer tests where Y_0 [m] is the cumulative amount of percolation related to the application period. Then outflow concentration C_1 [kg m^{-3}] from mixing layer describes the mass balance within mixing layer (Fig. 1) where the solute transport is determined by advective transport and sorption processes (Eq. 4).

$$d_1\ (\theta_1 + \rho_b\, K_a)\ \frac{\partial C_1}{\partial t} = q\, C_0 - q\, C_1 \tag{4}$$

where d_1 [m] is the depth. The solution of Eq. (4) for the initial condition $C_1(0)=0$ is split into the following two cases:

$$0<t\leq T_0{:}C_1(t)=C_0\left(1-\exp\left(-\frac{Y}{W_a}\right)\right)$$
$$t>T_0{:}C_1(t)=C_0\left(1-\exp\left(-\frac{Y_0}{W_a}\right)\right)\exp\left(-\frac{Y}{W_d}\right) \tag{5}$$

The solution for $0<t\leq T_0$ refers to the application phase when the reservoir of the mixing layer is being filled and basically adsorption takes place. The solution for $t\geq T_0$ corresponds to the leaching phase from the reservoir with the concentration $C_1(T_0)$ and desorption is taking place. Different partitioning coefficients for adsorption (K_a) and desorption (K_d) represent possible hysteresis. The W_a and W_d are defined as apparent water content (Steenhuis et al., 1994):

$$W_a = d_1\ (\theta_1 + \rho_b\, K_a)$$
$$W_d = d_1\ (\theta_1 + \rho_b\, K_d) \tag{6}$$

Since sorption is neglected within the transport layer, the transport is considered only as "preferential" flow. The volumetric water content θ_2 represents only the mobile water phase which is defined as preferential flow. The mass balance in this layer is determined only by the inflow concentration C_1 (Fig. 1). Therefore, the outflow concentration C_2 is determined by:

$$0 \le T_2 : C_2(t) = 0$$
$$t > T_2 : C_2(t) = C_1\,(t - T_2) \tag{7}$$

where the mean transport time T_2 in transport layer is defined by:

$$T_2 = \frac{W_2}{q} \tag{8}$$

The apparent water content of the transport layer depends only on the depth d_2.

$$W_2 = d_2\,\theta_2 \tag{9}$$

The overall transport is quantified by the mass leaching monitored at the system outflow by means of the outflow concentration C_2 of the transport layer. Mass balance is described by calculating the deficit of the mass recovery on a logarithmic scale

$$\ln\left(1 - \frac{L(Y)}{M_0}\right) \tag{10}$$

where $L(Y)$ defines the mass loss from the system in terms of cumulative percolation Y

$$L(Y) = \int_0^t q\, A\, C_2(t')\, dt' = \int_0^Y A\, C_2(Y')\, dY' \tag{11}$$

and $M_0 = A\ q\ C_0\ T_0$, the total injected solute mass to cross section area A [m^2] in the time interval T_0, which is defined by the observed concentration $C_2(T_0) = C_1(T_0 - T_2)$

$$T_0 = T_2 + T_1 = \frac{W_2}{q} - \frac{W_a}{q} \ln\left(1 - \frac{C_1(T_1)}{C_0}\right) \tag{12}$$

There are two calculations of the integral Eq. (11) necessary due to the two different solutions for $C_1(t)$ (see Eq. 5), since the outflow concentration $C_2(t)$ has to be expressed by $C_1(t)$. This requires a time shift of T_2 for the formulation of time depending function and the integration boundaries. Hence, the mass loss $L(Y)$ can be expressed by:

$$\begin{aligned}
&0 \le Y \le Y_2: && L(Y) = 0 \\
&Y_2 < Y \le (Y_0 + Y_2): && L(Y) = A\, C_0 \int_{Y_2}^{Y} \left(1 - \exp\left(-\tfrac{Y' - Y_2}{W_a}\right)\right) dY' \\
&Y > (Y_0 + Y_2): && L(Y) = A\, C_0 \int_{Y_2}^{Y_0 + Y_2} \left(1 - \exp\left(-\tfrac{Y' - Y_2}{W_a}\right)\right) dY' + \\
& && \quad A\, C_0 \int_{Y_0 + Y_2}^{Y} \left(1 - \exp\left(-\tfrac{Y_0}{W_a}\right)\right) \exp\left(-\tfrac{Y' - Y_0 - Y_2}{W_d}\right) dY'.
\end{aligned} \tag{13}$$

HESSD
6, 5631–5664, 2009

Calculating the integrals in Eq. (13) and substituting into Eq. (10) gives the deficit of the mass recovery:

$$
\begin{aligned}
0 \le Y < Y_2 : \quad & \ln\left(1-\frac{L(Y)}{M_0}\right) = 0 \\
Y_2 \le Y < (Y_0+Y_2) : \quad & \ln\left(1-\frac{L(Y)}{M_0}\right) = \ln\left[1-\frac{Y-W_a}{Y_0}+\frac{W_a}{Y_0}\left(1-\exp\left(-\frac{Y-W_2}{W_a}\right)\right)\right] \\
Y \ge (Y_0+Y_2) : \quad & \ln\left(1-\frac{L(Y)}{M_0}\right) = \ln\left[\left(\frac{W_a}{Y_0}-\frac{W_d}{Y_0}\left(1-\exp\left(-\frac{Y-W_2-Y_0}{W_a}\right)\right)\right)\left(1-\exp\left(-\frac{Y_0}{W_a}\right)\right)\right]
\end{aligned}
\tag{14}
$$

Equation (14) was implemented within a spreadsheet for investigation of the shape of the leaching curves in response to varying parameters for conceptually two different systems. In this parameter study, K_a and K_d coefficients, depth of distribution layer, d_1 and its water contents θ_1 and depth of transport, d_2, and its water contents θ_2, and the ratio C_1/C_0 at the end of application T_0 varied (Table 1). The resultant response as mass loss curve is noted under two scenarios: (i) System-I, a homogeneous soil (the mixing layer and the transport layer has the same water contents), and (ii) System-II, a two-layered soil with distinguished soil properties and fixed layer depth where the transport layer has preferential flow and no adsorption.

Line #R0 in Fig. 2 represents a set of reference parameters for System-I with d_1=10 cm, d_2=38 cm, $\theta_1=\theta_2$=0.35, $K_a=K_d$=0 and C_1/C_0=0.97. An increase in the depth of the mixing layer over #R0 results in a decrease of slope of leaching phase (#01, #02, #03) due to more mass stored. The variation of the application time (#04, #05) defined by the ratio C_1/C_0 shifts the falling limb due to successively less mass being applied. Greater water content over #R0 delays the mass recovery (#06) due to the more mass stored, and the lesser water content (#07, #08, #09) accelerates the mass recovery due to the less mass stored. An increase of sorption over #R0 delays and slows down the mass recovery (#10). An additional lesser K_d than K_a results in strong tailing of the mass recovery increasing with magnitude of differences of the coefficients (#11, #12).

In System-II, increasing the proportion of preferential flow by lowering the water content in transport layer resulted in earlier mass recovery (#13). Further lesser water

content in the mixing layer (#14 and #15) enhanced the effect. Variation of sorption properties of the two layered soil, when preferential flow existed, yielded early recovery compared to the homogeneous system with same K_a/K_d values (compare #10 and #16) and a successively delayed recovery with increasing K_a (#17, #18).

3 Materials and methods

This tracer study comprised 16 undisturbed columns taken from four soils ranging in texture from loamy sand to silty clay and in structure from massive to well-developed firm subangular and prismatic. Lithium chloride was applied for 1 to 2 PV and leached with synthetic rain water at four constant flow rates. Percolate concentrations of the tracers were fitted to the transport equations (Eqs. 1, 3 and 14). Comparative fit of the equations and the parameters' variability were examined on the basis of variability in soil structures and flow regimes.

3.1 Site description

All the four soils included in the tracer study were "Parabraunerde" in German soil classification system located in SW-Germany (Regierungspräsidium Karlsruhe, 1999). The parallel US class names are: (i) Lamellic Hapludalf, massive to weak coarse subangular blocky loamy sand; (ii) Lithic Hapludalf, moderate medium and coarse subangular blocky silt clay loam; (iii) Typic Udorthent, granular (surface layer) and moderate medium and coarse subangular blocky silty clay loam; and (iv) Typic Hapludalf, strong medium subangular blocky and prismatic silty clay. All the soils are moderately to well drained and occur in udic moisture regimes (mean annual rainfall 700 to 850 mm). At all sites forest dominates the land use.

Lamellic Hapludalf has developed in fluvial sand with massive to weak coarse subangular blocky loamy sand Al (2–20 cm) surface of pH 4.4 and massive sand Bv (20–50 cm) subsurface with pH 4.7. The Lithic Hapludalf has developed in limestone cov-

ered by glacial loess of last ice age. It has moderate medium granular silt loam Ah (0–4 cm) surface pH 4.7; moderate medium and coarse angular blocky silt loam Bv-Al (4–25 cm) horizon pH 6.0; and moderate coarse subangular blocky silty clay loam Bt (25–48 cm) horizon pH 6.5. The Typic Udorthent is developed in intact loess in a hilly surrounding of the Kraichgau region with granular silt loam Ah (0–6 cm) surface of pH 5; weak to moderate medium and coarse subangular blocky and platy silt loam Al (6–20 cm) of pH 4.2; moderate medium and coarse subangular blocky silt loam Bt (20–63 cm) horizon of pH 5.0. The Typic Hapludalf is developed on Upper Muschelkalk in a local colluvial position. It has granular and medium subangular blocky silt loam Ah (0–4 cm) surface pH 5.4; moderate medium angular blocky silty clay loam, pH 4.95 Bv-Al horizon (4–25 cm); and strong medium subangular blocky and prismatic silty clay, pH 6.2 Bt horizon (25–55 cm).

3.2 Soil column preparation and leaching experiments

Four intact columns were excavated from each site and fixed in 36 cm inner diameter and 50 cm long polyethylene drainage pipes using expanding polyurethane foam. The column base was fitted with a drainage chamber and saturated slowly by raising water table. Leaching experiments were carried out at four constant flow rates controlled by (i) +10 mm water head for saturated flow using Mariotte bottle-fed system, and (ii) −10 mm water head, (iii) −40 mm water head, and (iv) −100 mm constant water heads at the column surface using a tension infiltrometer. Negative water heads were intended to control magnitude of inflow ("unsaturated flows") rather than to create matric potential regimes through out the soil column length. We were conscious that the matric potential may have been prevented due to the capillary fringes. A tension infiltrometer design of Perroux and White (1988) and Simunek et al. (1998) was modified to accommodate a large porous plate and reservoir. Lithium chloride (3.5 mM) was prepared in tap water and adjusted to pH 5.5.

Chronologically, experiments started with leaching at −40 mm water head. Constant flow at −40 mm water head was achieved using synthetic acid rain (pH 5.5) and then

application phase started by switching LiCl solute. With Chloride concentration ratio in the percolate approaching one, the flow to the porous disc was switched back to solute free synthetic acid rainwater (flushing phase). Leaching was repeated at −10 mm and −100 mm water heads using the same columns. Each time the constant flow rate was obtained with acid rain at respective suction head before the tracer application. Leaching at constant +10 mm ponding was carried out between −10 and −100 mm water heads. The leachate was collected during both the application and flushing phases and frequency of sampling was with the outflow rate.

3.3 Sample analysis

Chloride in percolate was measured using ion selective electrode and later acidulated by adding 200 μL HNO_3 per 100 mL solution, filtered through 0.45 μm nominal porosity screen, and stored at 4°C until analysis. Lithium was measured using Atomic Absorption Spectrophotometer (AAS). Chloride and Lithium concentration ratios were plotted against the drainage depth for each leaching.

3.4 Convective-dispersive-equation fitting

The breakthrough data were fitted to two-region CDE in inverse mode employing STANMOD, a Windows based computer code (Simunek et al., 1999) which uses analytical solutions of deterministic non-equilibrium CDE (Toride et al., 1999) where input data consisted of solute concentration ratio and drainage depth [m] as proxies for solute concentration and time, respectively. The boundary conditions included characteristics length of 0.48 m and total input pulse equal to the drainage depth for application phase and the initial condition that constant concentration of Chloride (equal to concentration of tap water) leaches through the column. Further, as the rain used for flushing contained detectable Chloride, two input pulses were used: the first pulse had the input concentration of 1 for the duration (drainage) of application phase and the second pulse had the input concentration equal to Chloride in tap water. No decay or

production terms were included.

For each experiment uniqueness of optimised parameters was verified by repeated runs varying initial values of parameters (Langner et al., 1999). An analytical solution was accepted once the highest goodness of fit (r^2) and dispersivity (D/v) 2 cm<D/v<20 cm, mean square error for model <0.01, and T-value on parameters ≥1. The predicted parameters for Chloride were: velocity of the mobile region, v_m, defined as $\theta/\theta_m \times v$ [m m^{-1}] dispersion in mobile region, D_m, defined as $\theta_m/\theta \times D$ [m^2 m^{-1}] water partitioning coefficient, β, θ_m/θ and mass transfer function, ω. Assuming the v_m for Cl' represents the pore water velocity and given the drainage as a proxy for time, inverse of v_m represents the effective porosity θ_e or quantum of preferential flow. Mobile water fraction is then $\theta_m = \beta \times 1/v_m$ (Cl). Retardation of Lithium was predicted from the pore water velocity.

3.5 Preferential flow equation fitting

Chloride and Lithium breakthrough data were fitted to simple and modified preferential flow models, i.e., Eqs. (3) and (14), respectively. Equation (3) was a linear regression between ln(1-L/M_0) and cumulative drainage, Y, without an intercept (Akhtar et al., 2003b) and inverse of slope yielded apparent water content, W. In a spreadsheet, the Eq. (14) was superimposed on the scatter plot of ln(1-L/M_0) versus Y for Chloride adjusting the analytical solution to overlay by repetitively substituting values for W_a, W_d and W_2 coefficients until the highest correlation coefficient r^2 was achieved. The depths of the mixing and distribution layers (d_1 and d_2) were the observed horizons for each soil. Concentration $C_1(T_0)$ and flow rate, q were known for each leaching experiment. Total depth of the soil column, h was set to 0.48 m and bulk density, ρ_b to 1.32 Mg m^{-3}. Specific flow rate q does not affect since the application time was determined by ratio C_1/C_0. Water contents (θ_1, θ_2) could be derived from the fitted parameter W_a, W_d, and W_2 because of the conservative behaviour of Cl (K_a=K_d=0). For Lithium fit, d_1, d_2, θ_1, and θ_2 remained as those for Chloride and only K_a and K_d coefficients were substituted

until the highest r^2 with the plot of ln(1-L/M_0) vs. Y was achieved. Finally, R for Li^+ was calculated by Eq. (2).

4 Results

This section includes brief description of Chloride and Lithium breakthrough curves as affected by soil structure and water head; fit of the breakthrough data by the CDE and relationship of transport parameters with flow conditions, and finally, fit of the same data according to Eqs. (3) and (14) is presented.

4.1 Chloride and lithium breakthrough

Type of soil structure and the flow rate resulted in variation in arrival of Chloride and Lithium and peak concentration ratio (Fig. 3). More detailed description of breakthrough and transport parameters by fitting two-domain CDE was separated previously (Akhtar et al., 2009). Briefly, Chloride in the massive loamy sand (Lamellic Hapludalf) arrived after approximately 0.5 PV (8 to 10 cm drainage), and CDE simulated velocity (v_m) of 2.8 to 3.8 cm cm^{-1} drainage, dispersion (D_m) 4 to 8 cm^2 cm^{-1} drainage, and water partition coefficient (β) of 0.85 to 0.95 suggesting dominant matrix flow over all the flow rates (Fig. 3a). Chloride breakthrough in most columns from the well-structured silty clay soils occurred within a few cm drainage under ponded flow (+10 mm water head) with CDE simulated v_m between 10 to 20 cm cm^{-1} drainage, dispersion front of 40 to 220 cm^2 cm^{-1} drainage, and water partition coefficient (β) of 0.25 to 0.75, and the low flow rates controlled by successive negative water head, resulted in delayed breakthrough (Fig. 3b,c), reduced v_m, decrease in D_m, and increase in β.

Relative concentration of Lithium in the percolate was lower than that of Chloride and the difference increased with decrease in flow rate. In the Lamellic Hapludalf breakthrough occurred between 18 and 22 cm of drainage for all the flow rates, rise in concentration with cumulative drainage was uniform (Fig. 3d), and retardation of

Lithium remained between 2 and 5 times that of Chloride. In all the structured silty clay loam/silty clay columns at saturated flow rate (+10 mm water head) Lithium appeared in the outflow as fast as Chloride and the maximum C_1/C_0 reached 0.80 to 1.0 within 5 cm of drainage (Fig. 4e). In the Typic Udorthent columns although breakthrough of Lithium at saturated flow was most immediate and concentration increase was faster than the Lithic Hapludalf and Typic Hapludalf (Fig. 3e,f), but as the flow rates decreased under −10 mm water-head (and more negative) the decrease in maximum Lithium concentration was more than other silty clay soils. Retardation of Lithium in the structured silty clay columns remained between 2 and 5 times that of Chloride under ponded flows, and as the flow rate decreased the retardation increased to between 10 and 20 times that of Chloride.

4.2 Preferential flow model fit

Figure 4 depicts Chloride and Lithium mass loss in the soil columns as a function of cumulative drainage at the flow rates controlled by +10, −10, −40 and −100 mm water-heads at column surface. If Eq. (3) is valid, the data will plot as a straight line without intercept. Except for the initial nonlinear part, comprising of few cm to few tens cm drainage, overall the data did plot as straight line for the cases where macropore flow was dominant (well structured silty clay columns). The initial drainage depth for which the data plotted nonlinear reflect interaction with the matrix. Interaction was in case of matrix type flow either due to absence of macropores (loamy sand) or due to lack of access to the macropores (−40 and −100 mm water heads even in the well structured soils). The initial nonlinear plots for Lithium data extended for a greater drainage depth compared to those for Chloride in all the soils especially in the Lamellic Hapludalf.

After the initial nonlinear part, solute remaining in the columns fitted the straight line with widely differing slopes due to variation in percolate. Mass loss with the flow rate at +10 and −10 mm water heads plotted with steeper slope than those at −40 and −100 mm water heads. In the Typic Unorthent column with biological pores visible at the surface and in the Typic Hapludalf columns with structural macropores (which

caused immediate breakthrough at saturated flow), the solute remaining in soil fitted almost a straight line with the steepest slope. The Typic Unorthent columns had the slowest breakthrough at −100 mm head and the fastest at +10 mm water head and resulted in a wider variability in the slopes of lines both for Chloride (Fig. 4 left) and Lithium (Fig. 4 right).

All the data in Fig. 4 was fitted to Eq. (3), but only selected lines are plotted against drainage to depict better fit in case of macropore flow and poor fit in case of dominant matrix flow (Fig. 5). Overall the data did plot on a straight line but with an optimal fit only at +10 mm water head in the Typic Hapludalf (r^2 0.98) when macropore flow was dominant (Fig. 5a, b). Due to high interaction with the matrix, straight line fit was poor with r^2 0.89 for Chloride and 0.81 for Lithium in the same soil under unsaturated condition when matrix flow was relatively dominant. On the other hand, in the Lamellic Hapludalf soil where matrix type flow was dominant both at +10 mm and −100 mm water heads, the straight line fit was less than optimal for both the solutes (Fig. 5c, d). Since the Eq. (3) assumes instantaneous mixing, it also failed in the initial part when tracer was being applied into the continuous water flow, and outflow concentration was increasing. Therefore, in this situation slope of the straight line did not represent the true slope of data not only when the matrix flow was dominant (interaction with matrix in vadose zone) but also when the assumption of instantaneous mixing was violated. Apparent water content (W) for the selected data is also included in Fig. 5 which might be inaccurate when solute was carried through soil macropores.

Equation (14) did not have assumption of instantaneous mixing and it fitted well in almost all cases. Solid lines in Fig. 6 depict high fit for the same data sets as in Fig. 5. Here r^2 was as high as 1.00. Apparent water content from Eq. (14) was approximately 50% less than that obtained from Eq. (3) for the same data (compare W and W_a for respective solute given within the legends in Figs. 5 and 6, respectively). In Table 2 complete data for the adsorbing and nonadsorbing solutes fitted to the Eq. (14) is presented. Equation (14) fitted with high degree of fitness as indicated by high mean (n=4) r^2 and low σ on r^2. The mean W_a for Chloride varied between 4 to 8 cm for

leaching at saturated flow, and only slightly increased (6 to 12 cm) for unsaturated flow. Due to retention of the adsorbing solute, W_a for Lithium remained greater than that for Chloride in each soil and increased several fold for each decrease in water head in the silty clay loam/silty clay soils, while only two fold increase in case of Lamellic Hapludalf soil columns. Large preferential flow at saturation resulted in less W_a in well structured silty clay loam/silty clay soils than the massive loamy sand. Also, very low values of W_2 for the transport layer were obtained for all soils except Lamellic Hapludalf.

Lithium retardation (Eq. 2) for these four soils at various water heads was calculated by ratio of the fitted values W_a (Eq. 14) for Cl and Li assuming that Cl has no retardation (K_a=0) and d_1 and θ_1 are equal for Cl and Li. At saturated flow (+10 mm water head) retardation coefficient of the well structured silty clay soils was between 1.5 and 4 compared to 8 to 10 of the unstructured loamy sand soil. Increase in R of Lithium at unsaturated flow (−40 and −100 mm water heads) was several fold in the silty clay soils than the loamy sand soils, but the individual columns exhibited variability.

5 Discussion

Firstly, the combination of soil types and the water heads at column surface created meaningful variability in the measured flow rates (Table 2) and hydrologically determined effective saturation (Fig. 7). Effective porosity (θ_e), an inverse of pore water velocity, cm cm^{-1}, calculated by two-domain CDE is a better measure of fractional soil volumes contributing to the preferential flow compared to $\theta(h)$ relation. The $\theta(h)$ relation has high variability and hysteresis at high water contents (Langner et al., 1999). As the volume fraction of soil participating in flow processes, θ_e values below total porosity of 0.50 indicate magnitude of bypass flow (Rasmussen et al., 2000; Perfect et al., 2002; Chen et al., 2005). In this study θ_e varied in a narrow range of 0.25 to 0.33 under all the flow rates in the massive loamy sand Lamellic Hapludalf soil (dominant matrix type flow) and 0.05 under ponding of 10 mm water, increased to 0.15 with reduced flow in the structured silty clay soils θ_e.

Secondly, we are conscious of the question of uncertainty of achieving designated potential and the fact that it is impossible to obtain uniform matric potential throughout the column length (ascribed to rise in capillary fringe controlled by pore size distribution) without external suction at the outflow end (Rasmussen et al., 2000). It is further assumed that the solute leached under rapid pressure head associated with macropore flow (Germann and Di Pietro, 1999), and the kinematic pressure wave pushed existing water out of soil column (Rasmussen et al., 2000). Rise in capillary fringe was not noticed in soils with macropores (Williams et al., 2003). Nevertheless, installation of a tensiometer in column could have indicated in vitro water potential provided contact and sufficient equilibrium time are insured (Hutchison et al., 2003).

The solute remaining in the columns fitted on a straight line only after an initial nonlinear part and with widely differing slopes. A straight line fit in similar well structured soils associated macropore flow and curvilinear fit in dominant matrix flow through massive loamy sand soil have been reported previously (Akhtar et al., 2003b). In this study, the same data from the loamy sand also fitted straight line after the initial nonlinear part. In the study of Akhtar et al. (2003b) solute sampling continued after flushing cycle had stopped which resulted in unsteady state flow due to continuous increasing desaturation compared to the constant flux here. Consequently, the solute concentration remained high for a larger drainage depth when travel time from the mixing zone to the bottom of the columns increased due to matrix flow. A longer initial nonlinear plot for Lithium data compared to Chloride in all the soils was due to the sorption processes. The Typic Udorthent had wider differences in slopes and corroborated with differences in the breakthrough curves. It had the slowest breakthrough at −100 mm and fastest at +10 mm water heads (Fig. 4b).

Violation of the assumption of instant mixing and interaction of solutes within the transport layer caused failure of Eq. (3) in case of dominant matrix flow both in massive soil and at low flow rate in the well-structured silty clay columns. Thus, while for the Typic Hapludalf no exchange of solute took place between macropore and matrix especially at high flow rates – which is assumed in the preferential flow model (Steenhuis

et al., 1994) – resulting in a better fit to straight line (Eq. 3) in case Typic Hapludalf (Fig. 5), surprisingly for the same data sets the modified form of the preferential flow model (Eq. 14) fitted very well for a large number of data sets (Fig. 5 as an example). The level of fit appeared to be independent of soil type or saturation (Table 2).

Apparent water content (W_a) which represents water requirement for leaching 50% of mass of solute applied, varied between 4 to 12 cm for Chloride (only slightly increased for unsaturated flow in all soils; Table 2). Apparent water content (W_a) was several fold greater for Lithium which increased with decrease in water head in the silty clay loam/silty clay soil. This concurs with an increased interaction and retention of the adsorbing solute. Interestingly yet, the same soils had W_a for Lithium close to that of Chloride when saturation was high and flow was fast. Further, it is obvious that the retardation potential is a dynamic property of a soil and depends upon saturation during the transport process, i.e. a greater retardation with decrease in saturation caused greater interaction with matrix and vice versa. Then, the validity of the adsorption coefficient determined from the batch experiments remains in questions for application in field soil conditions.

Finally, comparison of the conventional CDE and the preferential flow equations can be made through the retardation values obtained by these two independent modeling approaches (Fig. 8). Figure 8 was plotted on log scale to distribute magnitude of error over magnitude of value. It shows a good correlation coefficient, r^2 between retardations (R) determined by two independent methods. It also suggests that both the models gave almost identical values at various water heads – less at +10 and −10 mm water heads and more for −40 and −100 mm water-heads. It is interesting that with the simplicity (far few parameters are needed to fit the data) the modified preferential flow equation gave remarkably close values for the retardation of the adsorbing solute.

6 Related experiments

Finally, it is of interest to compare these results with related work on undisturbed cores or the field soils. Field application of blue dye (FD&C Blue #1) marked vertical fingers in the massive loamy sand soil (Lamellic Hapludalf) and macropores in the well structured soils where the lowest dyed area and the deepest penetration was associated with a strong angular blocky and prismatic structures of the Typic Hapludalf. Spreading of blue dye perpendicular to the macropores in weak and moderate subangular blocky Lithic Hapludalf and Typic Udorthent may suggest porosity of macropore walls. X-ray tomography of intact soils columns from these four soils revealed fairly well connected pores in the Typic Hapludalf and Typic Udorthent and fewer number limited in upper 35 cm, in the Lithic Hapludalf which also had large voides (krotovinas) loosely filled with low density material (soil organic matter, etc). The Typic Udorthent showed relatively fewer macropores than Lithic Hapludalf and Typic Hapludalf but appeared well connected. The Typic Hapludalf had the highest number of macropore per unit area which appeared well connected at the resolution examined.

7 Summary and conclusions

We are suggesting a modified preferential flow equation that has been tested using Chloride and Lithium breakthrough at constant flows. Constant flows were generated by +10 mm, −10 mm, −40 mm, and −100 mm water-heads at the surface of four columns from each of four soils which exhibited either dominantly finger flow or macropore flow. Preferential transport of solute was evident in all columns with rapid appearance of both nonadsorbed Chloride, and at lower peak concentrations, Lithium. Despite great differences between individual columns, the overall pattern of solute loss was very similar between columns when variable preferential flow effects dominated. The similarity in overall loss is a direct consequence of the drainage water concentration being a function of the amount of solutes in the distribution layer. Lack of in-

stantaneous mixing caused the simple preferential flow model (Steenhuis, 1994) fail to simulate the data in most cases except where the macropore flow was highly dominant, the modified preferential flow equation despite fewer parameters, fitted well and yielded retardation coefficient for the adsorbing solute comparable with that determined by tow-domain CDE with r^2 0.95. The modified preferential flow equation when tested for other data set may provide alternative bases for modeling chemical transport in soil.

References

Ahuja, L. R., Rojas, K. W., Hanson, J. D., Shaffer, M. J., and Ma, L.: The Root Zone Water Quality Model. Water Resources Publications, LLC, Highlands Ranch, CO, 372 pp., 2000.

Akhtar, M. S., Stüben, D., and Norra, S.: Soil Structure and Flow Rate Control on Molybdate, Arsenate, and Chromium(III) Transport through Field Columns, Geoderma, in review, 2009.

Akhtar, M. S., Richards, B. K., Medrano, P. A., deGroot, M., and Steenhuis, T. S.: Dissolved phosphorus from undisturbed soil cores: Related to adsorption strength, flow rate, or soil structure?, Soil Sci. Soc. Am. J., 67, 458–470, 2003a.

Akhtar, M. S., Steenhuis, T. S., Richards, B., and McBride, M.: Chloride and lithium transport in large arrays of undisturbed silty loam and sand loam soil columns, Vadose Zone J., 2, 715–727, 2003b.

Bauters, T. W. J., DiCarlo, D. A., Steenhuis, T. S., and Parlange, J.-Y.: Preferential flow in water repellent sands, Soil Sci. Soc. Am. J., 62, 1185–1190, 1998.

Bejat, L., Perfect, E., Quisenberry, V. L. Coyne, M. S., and Haszle, G. R.: Solute transport as related to soil sturcture in unsaturated intact soil blocks, Soil Sci. Soc. Am. J., 64, 818–826, 2000.

Bundt, M., Albrecht, A., Froidevaux, P., Blaser, P., and Flühler, H.: Impact of preferential flow on radionulcides distribution in soil, Environ. Sci. Technol., 34, 3895–3899, 2000.

Castigione, P., Mohanty, B. P., Shouse, P. J., Simunek, J., van Genuchten, M. T., and Santini, A.: Lateral water diffusion in an artificial macropore system: modeling and experimental evidence, Vadose Zone J., 2, 212–221, 2003.

Chen, G., Flury, M., Harsh, J. B., and Lichtner, P. C.: Colliod-Facilited transport of Cesium in variably saturated Hanford Sediments, Environ. Sci. Technol., 39, 3435–3442, 2005.

Elliot, J. A., Cessna, A. J., Best, K. B., Nicholaichuk, W., and Tollefson, L. C.: Leaching and

preferential flow of Clopyralid under irrigation: Field observations and simulation modelling, J. Environ. Qual., 27, 124–131, 1998.
Flury, M., Leuenberger, J., Studer, B., and Fluhler, H.: Transport of anions and herbicides in a loamy and a sandy soil, Water Resour. Res., 31, 823–835, 1995.
Germann, P. F. and Di Pietro, L.: Scales and dimensions of momentum dissipation during preferential flow in soils, Water Resour. Res., 35, 1443–1454, 1999.
Huber, R., Fellner, J., Doeberl, G., Brunner, P. H.: Water flows of MSW landfills and implications for long-term emissions, J. Environ. Sci. Health, Part A, Toxic/Hazardous Substance Environ. Eng., 39, 885–900, 2004.
Hutchison, J. M., Seaman, J. C., Aburime, S. A., and Radcliffe, D. E.: Chromate transport and retention in variability saturated soil columns, Vadose Zone J., 2, 702–714, 2003.
Hutson, J. L. and Wagenet, R. J.: An Overview of LEACHM: A process based model of water and solute movement, transformations, plant uptake and chemical reactions in the unsaturated zone, Chemical Equilibrium and Reaction Models, SSSAJ Special Publication, 42, 409–422, 1995.
Jarvis, N. J., Bergstorm, L., and Dik, P. E.: Modeling water and solute transport in macroporous soil. II Chloride breakthrough under non-steady flow, J. Soil Sci., 42, 59–70, 1991.
Ju, S. H., Kung, K. J. S., and Helling, C. S.: Simulating impact of funnel flow on contaminant sampling, Soil Sci. Soc. Am. J., 61, 427–435, 1997.
Jury, W. A., Gardner, W. R., and Gardner, W. H.: Soil physics, John Wiley & Sons, New York, 1991.
Kim, Y. J., Darnault, C. J. G., Bailey, N. O., Parlange, J.-Y., and Steenhui, T. S.: Equation for describing solute transport in field soils with preferential flow paths, Soil Sci. Soc. Am. J., 69, 1–10, 2005.
Langer, H. W., Gaber, H. M., Wraith, J. M., Huwe, B., and Inskeep, W. P.: Preferential flow through intact soil cores: Effect of matric head, Soil Sci. Soc. Am. J., 63, 1591–1598, 1999.
Lappala, E. G., Healy, R. W., and Weeks, E. P.: Documentation of computer program VS2D to Solve the Equations of Fluid Flow in Variably Saturated Porous Media, US Geological Survey- Water-Resources Investigations Report, 83-4099, p. 184, 1987.
Mahmood-ul-Hassan, M., Akhtar, M. S., Gill, S. M., and Nabi, G.: Simulation of chloride transport based on descriptive soil structure, Pak. J. Sci. Ind. Res., 46, 424–431, 2003.
Marshall, T. J., Holmes, J. W., and Rose, C. W.: Soil Physics, 3d ed. Cambridge University Press, 453 pp., 1996.

McIntosh, J., McDonnell, J. J., and Peters, N. E.: Tracers and hydrometeric study of preferential flow in large unduistrubed soil cores from the Georgia Piedmont, USA, Hydrol. Process., 13, 139–155, 1999.
Mohanty, B. P., Bowman, R. S., Hendrickx, J. M. H., and van Genuchten, M. T.: Preferential transport of nitrate to a tile drain in an intermittent-flood-irrigated field: Model development and experimental evaluation, Water Resour. Res., 34, 1061–1076, 1998.
Parker, J. C. and van Genuchten, M. T.: Determining transport parameters from laboratory and field tracer experiments, Virginia Ag. Exp. Station, Blacksburg, Bull. 84(3), p. 91, 1984.
Perfect, E., Sukop, M. C., and Haszler, G. R.: Prediction of dispersivity for undisturbed soil columns from water retention parameters, Soil Sci. Soc. Am. J., 66, 696–701, 2002.
Perroux, K. M. and White, I.: Designs for disc permeameters, Soil Sci. Soc. Am. J., 52, 1205–1215, 1988.
Quisenberry, V. L., Phillips, R. E., and Zeleznik, J. M.: Spactial distribution of water and chloride macropore flow in a well-structured soil, Soil Sci. Am. J., 58, 1294–1300, 1994.
Rasmussena, T. C., Baldwin, R. H., Dowd Jr., J. F., and Williamsd, A. G.: Tracer vs. pressure wave velocities through unsaturated saprolite, Soil Sci. Soc. Am. J., 64, 75–85, 2000.
Regierungspräsidium Karlsruhe, Landschaften und Böden im Regierungsbezirk Karlsruhe. E. Schweizerbart'sche Verlangsbuchhandlung, Stuttgart. Germany, 96 pp., 1999.
Ritsema, C. J. and Dekker, L. W.: How water moves in a water repellent sandy soil 2. Dynamics of finger flow, Water Resour. Res., 30, 2519–2531, 1994.
Sarmah, A. K., Close, M. E., Pang, L., Lee, R., and Green, S. R.: Field study of pesticide leaching in a Himatangi sand (Manawatu) and a Kiripaka bouldery clay loam (Northland). 2. Simulation using LEACHM, HYDRUS-1D, GLEAMS, and SPASMO models, Aust. J. Soil Res., 43, 471–489, 2005.
Shaw, J. N., West, L. T., Radcliffe, D. E., and Bosch, D. D.: Preferential flow and pedotransfer functions for transport properties in sandy Kandiudults, Soil Sci. Soc. Am. J., 64, 670–678, 2000.
Simunek, J., Angulo-Jaramillo, Schaap, M. G., Vandervaere, J. P., and van Genuchten, M. T.: Using an inverse method to estimate the hydraulic properties of crusted soils from tension disc infiltrometer data, Geoderma, 86, 61-81, 1998.
Simunek, J., van Genuchten, M. T., Sejna, M., Toride, N., and Leij, F. J.: The STANMOD computer software for evaluating solute transport in porous media using analytical solution of convection-dispersion equation. U.S. Salinity Laboratory Agri. Res. Service US Dept. Agri.

Riverside, California, 1999.
Steenhuis, T. S., Boll, J., Shalit, G., Selker, J. S., and Merwin, I. A.: A simple equation for predicting preferential flow solute concentrations, J. Environ. Qual., 23, 1058–1064, 1994.
Toride, N., Leij, F. J., and van Genuchten, M. T.: The CXTFIT code for estimating transport parameters from laboratory or field tracers experiments, Ver. 2.1. Res. Report No. 137. U.S. Salinity Laboratory Agri. Res. Service US Dept. Agri. Riverside, California, p. 121, 1999.
van Genuchten, M. T.: Recent progress in modeling water flow and chemical transport in the unsaturated zone, in: Hydrological interaction between atmosphere, soil and vegetation, IAHS Publ., 204, 169–183, 1991.
Vervoort, R. W., Radcliffe, D. E., and West, L. T.: Soil structure development and preferential solute flow, Water Resour. Res., 35, 913–928, 1999.
Vogel, H.-J., Cousin, I., Ippisch, O., and Bastian, P.: The dominant role of structure for solute transport in soil: experimental evidence and modelling of structure and transport in a field experiment, Hydrol. Earth Syst. Sci., 10, 495–506, 2006, http://www.hydrol-earth-syst-sci.net/10/495/2006/.
Wallach, R. and Steenhuis, T. S.: Model for Nonreactive Solute Transport in Structured Soils with Continuous Preferential Flow Paths, Soil Sci. Soc. Am. J., 62, 881–886, 1998.
Williams, A. G., Dowd, J.F., Scholefield, D., Holden, N. M., and Deeks, L. K.: Preferential flow variability in a well-structured soil, Soil Sci. Soc. Am. J., 67, 1272–1281, 2003.
Xue, S. K., Chen, S., and Selim, H. M.: Modeling alachlor transport in saturated soils from no-till and conventional tillage systems, J. Environ. Qual., 26, 1300–1307, 1997.
Zhang, D. X., Wallstrom, T. C., and Winter, C. L.: Stochastic analysis of steady-state unsaturated flow in heterogeneous media: Comparison of the Brooks-Corey and Gardner Russo models, Water Resour. Res., 34, 1437–1449, 1998.

Table 1. List of varied parameters in the parameter study.

#	h_1 [a]	h_2 (cm)	θ_1 [b]	θ_2	K_a [c]	K_d	C_1/C_0 [d]
R0, Ref. System I	10	40	0.35	0.35	0	0	0.97
01	20	30	0.35	0.35	0	0	0.97
02	30	20	0.35	0.35	0	0	0.97
03	40	10	0.35	0.35	0	0	0.97
04	10	40	0.35	0.35	0	0	0.90
05	10	40	0.35	0.35	0	0	0.80
06	10	40	0.40	0.40	0	0	0.97
07	10	40	0.30	0.30	0	0	0.97
08	10	40	0.20	0.20	0	0	0.97
09	10	40	0.10	0.10	0	0	0.97
10	10	40	0.35	0.35	0.5	0.5	0.97
11	10	40	0.35	0.35	1.0	0.5	0.97
12	10	40	0.35	0.35	1.0	0.5	0.97
13	10	40	0.35	0.20	0	0	0.97
14, Ref. System II	10	40	0.35	0.05	0	0	0.97
15	10	40	0.15	0.05	0	0	0.97
16	10	40	0.35	0.10	0.5	0.5	0.97
17	10	40	0.35	0.10	1.0	1.0	0.97
18	10	40	0.35	0.10	5.0	0.5	0.97

[a] h1 and h2, depth of mixing and transportation layers, respectively;
[b] θ1 and θ2, water content in the mixing and transportation layers, respectively;
[c] K_a and K_d, partitioning coefficient for adsorption and desorption, respectively; and
[d] C_1/C_0, concentration when flushing starts.

Table 2. Mean solute transport parameters determined by Eq. (14) (n=4 and standard deviation in parentheses).

Head	q	W2[a]	Chloride			Lithium		
			W_a^b	W_d^b	r^2	W_a	W_d	r^2
loamy sand Lamellic Hapludalf (massive)								
mm water	cm h^{-1}	cm				cm		
10	6.8(2.10)	6.25(2.3)	8.38(3.9)	5.88(1.0)	1.00(0.00)	68(30)	516(565)	0.98(0.01)
−10	2.1(0.34)	9.58(1.4)	6.25(2.3)	5.00(2.1)	1.00(0.00)	140(242)	255(498)	0.96(0.03)
−40	6.1(0.83)	7.30(3.4)	9.00(4.7)	4.23(1.9)	1.00(0.00)	19(7)	12(4)	0.99(0.01)
−100	0.6(0.16)	8.50(1.7)	7.78(1.5)	6.68(1.2)	1.00(0.00)	54(15)	398(461)	0.97(0.03)
silty clay Lithic Hapludalf (medium and coarse subangular blocky)								
10	23.5(23)	1.20(1.0)	7.88(3.7)	5.43(3.5)	0.99(0.01)	16(7)	7(3)	0.99(0.00)
−10	0.80(0.5)	1.88(1.0)	9.88(3.5)	4.30(3.0)	0.99(0.01)	102(36)	534(545)	0.99(0.01)
−40	0.64(0.4)	0.70(1.2)	9.93(1.5)	7.68(0.7)	1.00(0.00)	97(13)	88(40)	0.99(0.01)
−100	0.24(0.15)	1.38(0.7)	7.75(1.7)	6.13(1.1)	0.97(0.02)	142(129)	513(570)	0.97(0.03)
silty clay loam Typic Udorthent (medium and coarse subangular block)								
10	32(38)	0.10(0.0)	4.38(1.6)	3.00(1.9)	0.99(0.01)	7(3)	4.4(2)	0.99(0.01)
−10	0.8(0.40)	0.70(0.4)	6.98(2.4)	6.08(1.9)	1.00(0.00)	23(19)	64(96)	1.00(0.00)
−40	0.5(0.30)	3.40(2.8)	12.30(4.0)	10.20(3.9)	1.00(0.01)	610(938)	320(464)	0.94(0.11)
−100	0.1(0.02)	1.50(1.0)	11.75(1.0)	10.18(1.4)	1.00(0.00)	437(150)	1010(1)	0.93(0.04)
silty clay Typic Hapludalf (medium and fine blocky/prismatic)								
10	2.2(0.00)	1.00(0.7)	6.63(0.7)	4.00(2.0)	0.97(0.02)	22(7)	9(4)	0.99(0.00)
−10	1.4(0.20)	1.38(0.7)	12.13(1.2)	8.33(1.6)	0.99(0.01)	(5834)	38(20)	1.00(0.00)
−40	0.9(0.50)	2.25(1.0)	12.00(3.6)	10.75(2.6)	1.00(0.01)	117(89)	53(44)	1.00(0.00)
−100	0.1(0.04)	2.13(1.0)	10.55(3.0)	8.68(3.5)	1.00(0.00)	229(193)	402(444)	0.97(0.01)

[a] W_2, apparent water content of the transport layer (Eq. 9)
[b] W_a, apparent water content of the mixing layer (Eq. 6).

HESSD
6, 5631–5664, 2009

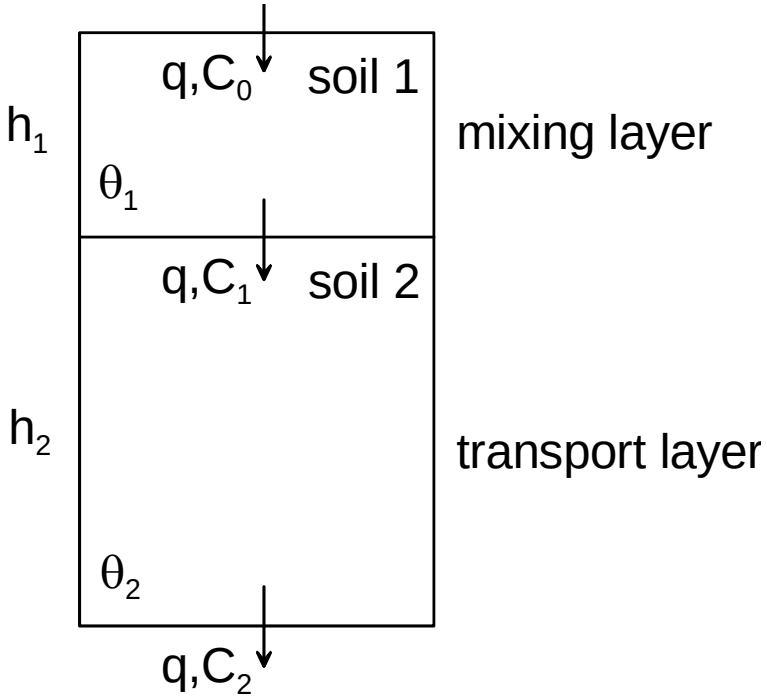

Fig. 1. Schematic representation of the two-layer approach as basis for simple preferential flow model for quantification of solute transport in soils.

HESSD
6, 5631–5664, 2009

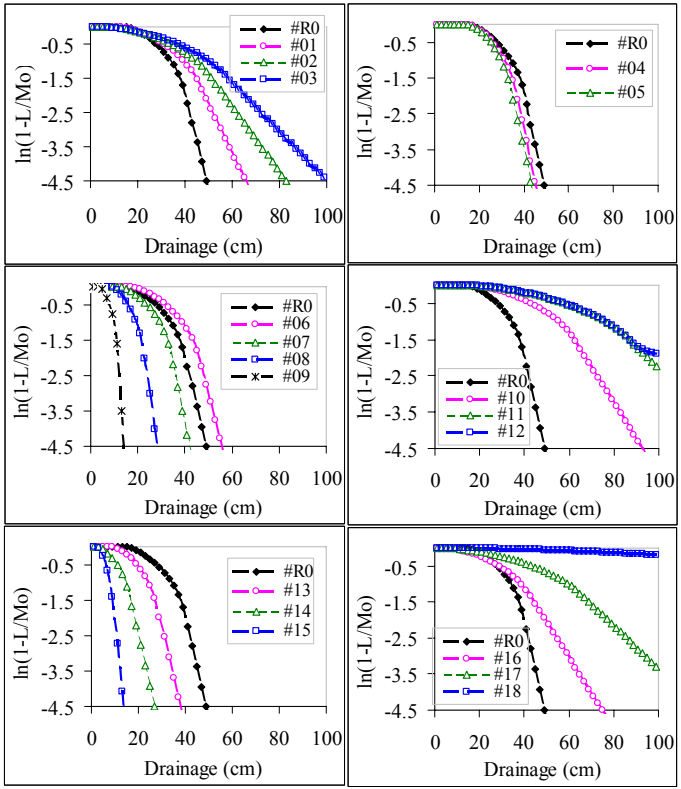

Fig. 2. Mass recovery deficit in dependence of the drainage depth determined using the parameters given in (Table 2).

HESSD
6, 5631–5664, 2009

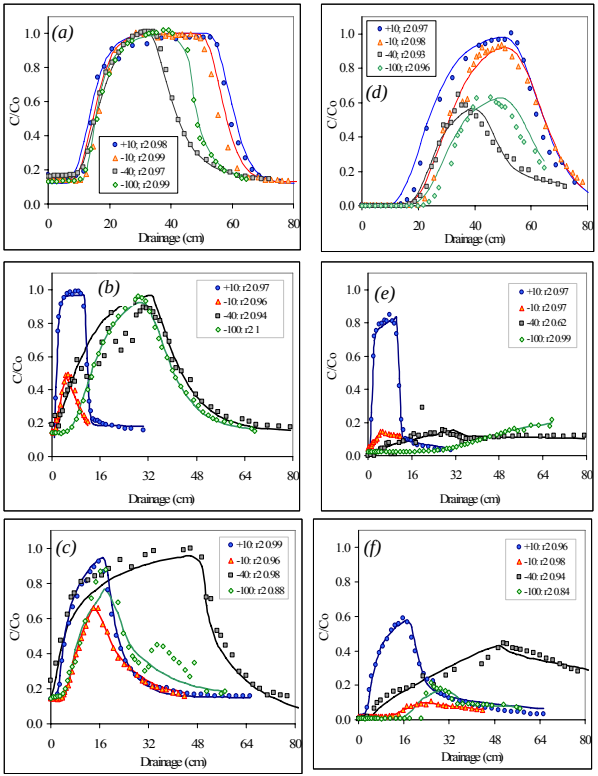

Fig. 3. Chloride and Lithium breakthrough in one representative columns from three selected soils: **(a)** Lamellic Hapludalf (column 4); **(b)** Typic Udorthent (column 4); and **(c)** Lithic Hapludalf (column 2); and **(d)**, **(e)**, and **(f)** depict Lithium breakthrough for the same columns. The solid line indicates fitted CDE and goodness of fit (r^2) given with the legend for the respective breakthrough.

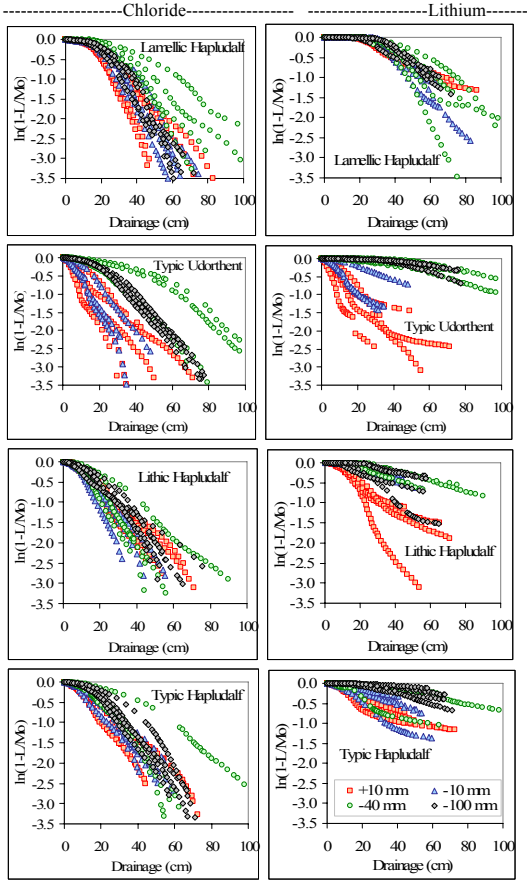

Fig. 4. Chloride (left) and Lithium (right) mass loss as a function of cumulative drainage: Lamellic Hapludalf, massive to weak coarse subangular blocky loamy sand; Lithic Hapludalf, moderate subangular blocky silt loam; Typic Unorthent, moderate coarse subangular blocky; and Typic Hapludalf, strong subangular blocky and prismatic silty clay.

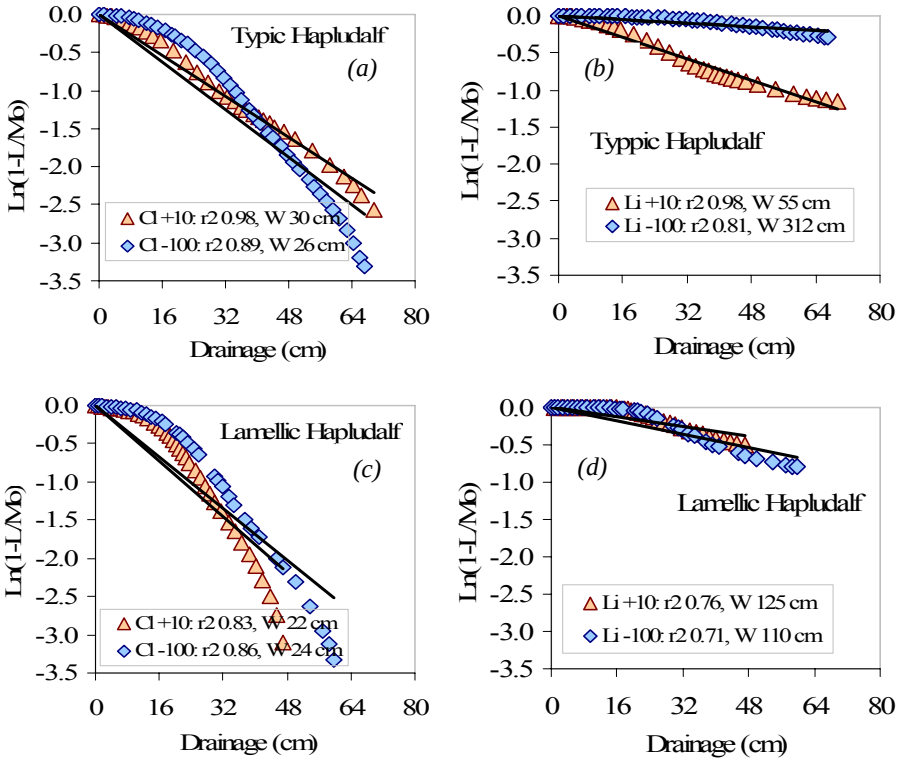

Fig. 5. Chloride and lithium breakthrough at high flow rate (+10 mm water) and low flow rate (−100 mm water heads): **(a)** and **(b)** for Chloride and Lithium, respectively, in the well structured silty clay Typic Hapludalf; and **(c)** and **(d)** for Chloride and Lithium, respectively in the massive loamy sand Lamellic Hapludalf. The solid line is the Eq. (3) and the fit and apparent water (W) given in legend.

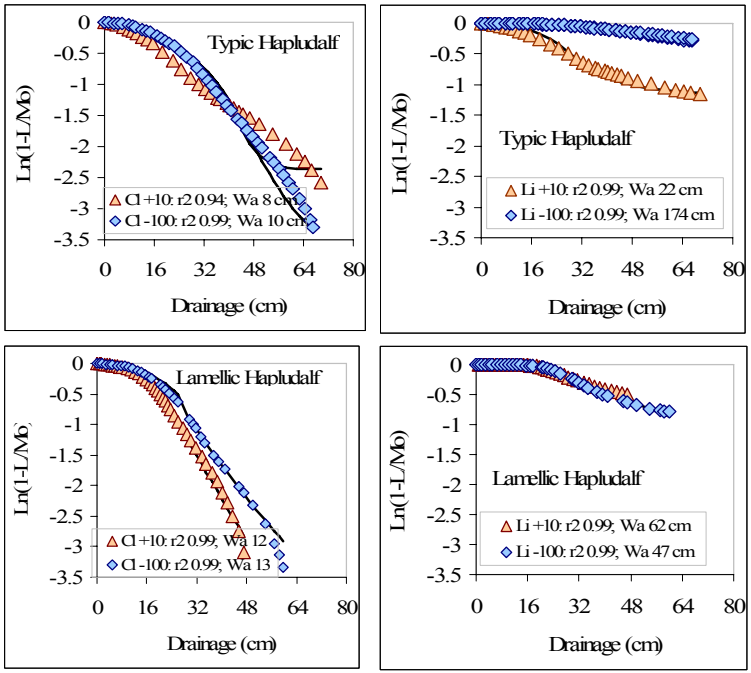

Fig. 6. Chloride and Lithium breakthrough at high (+10 mm) and low (−100 mm water head) flow rates: **(a)** and **(b)** for Chloride and Lithium, respectively for Typic Hapludalf, the well structured silty clay soil; and **(c)** and **(d)** for Chloride and Lithium, respectively for Lamellic Hapludalf, the massive loamy sand. The solid line is Eq. (14). The fit and apparent water (W_a) given in legend.

HESSD
6, 5631–5664, 2009

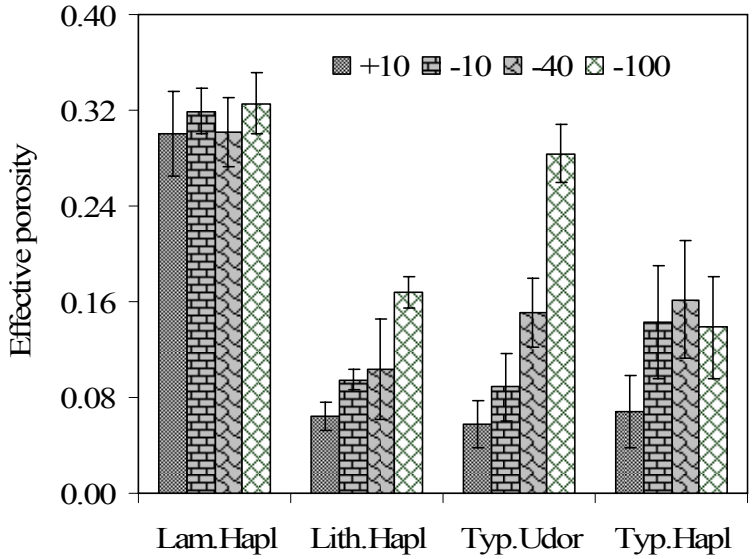

Fig. 7. Effective water content (θ_e, inverse of pore water velocity) determined by two-domain CDE.

HESSD
6, 5631–5664, 2009

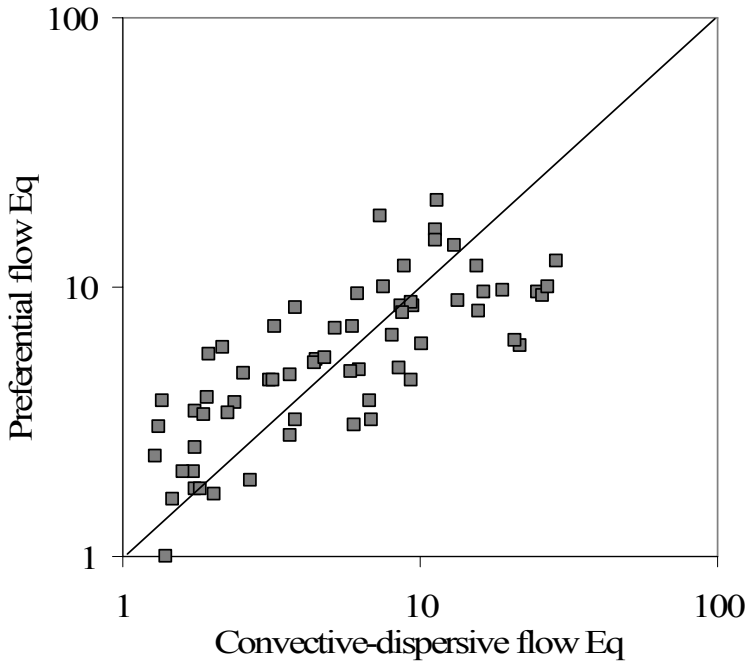

Fig. 8. Retardation coefficient obtained by the modified preferential flow model and CDE plotted on log scale (error magnitude distributed over magnitude of value).